2023 IEEE International Conference on Energy Technologies for Future Grids
Wollongong, Australia, December 3-6, 2023

2023 IEEE International Conference on Energy Technologies for Future Grids (ETFG) | 978-1-6654-7164-0/23/$31.00 ©2023 IEEE | DOI: 10.1109/ETFG55873.2023.10407319

Optimal Day-Ahead Scheduling of Distributed Energy Resources: A Strategy Based on Information Gap Decision Theory to Address Multiple Uncertainties in the Active Distribution Networks

Kasi Vemalaiah[1], *GSIEEE*, Dheeraj Kumar Khatod[1], *MIEEE*, and Narayana Prasad Padhy[1,2], *SMIEEE*
[1]Electrical Engineering Department, Indian Institute of Technology Roorkee, Roorkee, India.
[2]Director, Malaviya National Institute of Technology Jaipur, Jaipur, Rajasthan, India.
Email: {kasi_v, dheeraj.khatod, nppadhy}@ee.iitr.ac.in.

***Abstract*—The optimal scheduling of distributed energy resources within the distribution network improves the system's performance. Nevertheless, the inherent uncertainty associated with distributed energy resource output (especially renewable energy-based) and load demand poses a challenge when making optimal decisions. This paper proposes an information gap decision theory-based day-ahead scheduling scheme to maximize the robustness against multiple uncertainties having a lack of information. The uncertainties considered in this paper are photovoltaic generation and load demand. This framework quantifies how well a scheduling strategy performs in the presence of uncertainties by quantifying with a robustness function. Due to these multiple uncertainties, the proposed framework is formulated as a multi-objective optimization problem in the form of a mixed integer second-order cone program, which ensures a global solution. This scheme is implemented in GAMS software and solved using the GUROBI solver. To verify the effectiveness of the proposed framework, it is tested on a modified IEEE 33-bus distribution system. The results show that the proposed scheme is robust against multiple uncertainties and easy to implement with less computational time.**

***Index Terms*—Day-ahead scheduling, distributed energy sources, information gap decision theory, multiple uncertainties, robust scheduling.**

NOMENCLATURE

Indices	
k	Index for uncertainty parameter.
t	Index for time interval.
x, y	Index for bus.
xy	Index for branch.
Sets	
$\Omega/\Omega^{\mathrm{LD}}/\Omega^{\mathrm{MG}}$	Collection of network, load, and main grid buses.
$\Omega^{\mathrm{B}}/\Omega^{\mathrm{CB}}$	Collection of buses coupled withBESS/CB.
Ω^{PV}	Collection of buses with coupled with PV.
Υ	Uncertainty parameters set.
T	Time intervals set.
Parameters	
$\lambda_x^{\mathrm{ch}}/\lambda_x^{\mathrm{dis}}$	Efficiency of x^{th} BESS during charging/discharging.
$\mathcal{C}^{\mathrm{B}}/\mathcal{C}^{\mathrm{CB}}$	Operational cost of x^{th} BESS/CB.
$\mathcal{C}_t^{\mathrm{MG}}/k_q^{\mathrm{MG}}$	Active power purchase price of the main grid and its reactive counterpart.
$\overline{\gamma_{k,t}}$	Predicted value of k^{th} uncertainty parameter in t^{th} time interval.
$\overline{I_{xy}}$	Upper limit for current flowing in xy^{th} line.
$\overline{P_{x,t}^{\mathrm{LD}}}/\overline{Q_{x,t}^{\mathrm{LD}}}/\overline{S_{x,t}^{\mathrm{LD}}}$	Forecasted active/reactive/apparent power of x^{th} load at t^{th} time interval.
$\overline{P_{x,t}^{\mathrm{PV}}}$	Forecasted generation of x^{th} PV at t^{th} time interval.
$\overline{P_{xy}}/\overline{Q_{xy}}$	Upper limit for Active/Reactive power flowing in xy^{th} line.
$\overline{S_x^{\mathrm{B}}}$	Upper limit for BESS apparent power at x^{th} bus.
$\overline{V_x}/\underline{V_x}$	Upper/lower bound for voltage at x^{th} bus.
$\overline{N_x^{\mathrm{CB}}}/\overline{Y_x^{\mathrm{CB}}}$	Maximum number of acceptable switchings in a day/Maximum banks of x^{th} CB.
$\underline{\mathcal{E}_x^{\mathrm{B}}}/\overline{\mathcal{E}_x^{\mathrm{B}}}$	Lower/upper energy level limits for x^{th} BESS.
$\underline{P_x^{\mathrm{MG}}}/\overline{P_x^{\mathrm{MG}}}$	Lower/upper limits of active power for the main grid.
$\underline{Q_x^{\mathrm{MG}}}/\overline{Q_x^{\mathrm{MG}}}$	Lower/upper limits of reactive power for the main grid.
$\overline{Q_{x,step}^{\mathrm{CB}}}$	Step size of x^{th} CB.
Variables	
$\mu_{x,t}^{\mathrm{ch}}/\mu_{x,t}^{\mathrm{dis}}$	Binary variables associated with x^{th} BESS for charging/discharging.
$P_{x,t}^{\mathrm{ch}}/P_{x,t}^{\mathrm{dis}}$	Active power charge/discharge at x^{th} BESS.
$Q_{x,t}^{\mathrm{B}}/E_{x,t}^{\mathrm{B}}$	Reactive power/energy level at x^{th} BESS.
$\mu_{x,t}^{\mathrm{CB,UP}}/\mu_{x,t}^{\mathrm{CB,DN}}$	Binary variables associated with up/down regulation status of x^{th} CB.
$\tau_{x,t}^{\mathrm{CB}}$	Step status of x^{th} CB.
$Q_{x,t}^{\mathrm{CB}}$	Reactive power of x^{th} CB.
$P_{x,t}^{\mathrm{MG}}/Q_{x,t}^{\mathrm{MG}}$	Real/reactive powers of main grid(sub-station).
$V_{x,t}/\theta_{x,t}$	x^{th} bus voltage magnitude and angle.
$P_{xy,t}/Q_{xy,t}$	Active/reactive power flowing in xy^{th} line at t^{th} time interval.
$U_{x,t}/W_{xy,t}^{\mathrm{R}}/W_{xy,t}^{\mathrm{I}}$	Variables related to conic reformulation.
$\gamma_{k,t}$	k^{th} uncertainty parameter in t^{th} time interval.
δ_k	Uncertainty horizon of k^{th} uncertainty parameter.

This work is partially sponsored by the DST, India, through the research grants: ID-EDGe Project (DST-1390-EED), UI-ASSIST Project (IUS-1132-EED), D-SIDES Project (DST-1237-EED), and partially financed by SERB, India through research grant: Parameter and Topology Estimation of Distribution Network (SER-1667-EED).

I. INTRODUCTION

The incorporation of distributed energy resources (DERs), such as distributed generation, battery energy storage systems (BESSs), and capacitor banks (CBs), into existing distribution networks is transforming them into active distribution networks (ADNs). This evolution holds tremendous promise, with the integration of these DERs delivering many benefits to utility companies [1], [2] like peak load shaving, which reduces the stress on the system, reducing the curtailment of renewable energy sources by efficiently storing excess energy in BESS. Additionally, integrating DERs contributes to reducing energy losses, improving voltage profiles to maintain a stable supply, and opportunities for energy arbitrage by leveraging fluctuations in electricity prices [1], [2]. However, this significant shift towards an ADN architecture introduces a

new layer of intricacy and operational challenges. As a result, the quest for the optimal operation of ADNs in the presence of these active elements has garnered substantial attention from researchers.

The optimal sizing and operation of BESSs in the microgrid are presented in [3] to reduce the cost of operation. The optimal operation of BESS, along with renewable energy resources(RESs), is presented in [4]. The main objective of this work is to minimize the electricity cost by optimally dispatching BESSs and RESs. But to reduce the carbon emissions, the available generation from RESs should fed to the grid. The effectiveness of various convex power flow models of unbalanced distribution networks (DNs) integrated with BESSs are highlighted in [5]. The combined optimal scheduling and real-time dispatch of multiple BESSs in the real network is proposed in [6]. The optimal dispatch minimizes the operational cost, and real-time dispatch revises the dispatch of BESSs subjected to voltage violations by measuring the system state. In this work, the scheduling problem does not account for the uncertainty. Similarly, the combined day-ahead and real-time operation of BESSs in ADN is proposed in [7]. In this work, the uncertainty of photovoltaics (PVs) and load is modeled using probability-distributed functions (PDFs). The stochastic scheduling of BESS and CB in a day-ahead manner is discussed in [8]. This work models the optimization problem as a mixed integer second-order cone program (MISOCP), and uncertainty is modeled with PDFs. The stochastic model predicted control-based optimal operation of DERs is proposed in the work [9].

The generation from the RES is not accurate and majorly depends on the weather conditions. Similarly, load demand depends on weather conditions and residents' behavior at the distribution level [10]. So, an effective tool for addressing this uncertainty is required for decision-making purposes. Several methods are available in the literature to address the uncertainty from load demand and RESs, such as PDF, fuzzy membership function, uncertainty interval, etc. [11]. The historical data should be available for all these methods to model the uncertainty parameters. Information Gap Decision Theory (IGDT) is a decision-making framework used when there is uncertainty or ambiguity about key variables [12], especially when there is a lack of information about uncertainty. In IGDT, decision-makers aim to make robust choices against a wide range of possible scenarios or outcomes. It acknowledges that in complex, real-world scenarios, complete information may be lacking, and there can be gaps in one's knowledge. This IGDT framework has already been adopted in various power system research studies [13]–[16]. In [13], IGDT is used to model the uncertainty of natural disasters to improve DN resiliency. The optimal operation of the grid, considering the dynamic thermal rating of the transmission line, which depends on forest wildfires, is modeled using IGDT [14]. The security constraint unit commitment for optimal operation of the grid using IGDT is proposed in [15]. An optimal operation of DN using IGDT is proposed in [16], but the formulations are non-convex, which does not guarantee a global solution.

Based on the aforementioned discussion, this paper proposes a convex framework for the optimal operation of DERs for day-to-day operations, considering the multiple uncertainties. This framework is based on the context of an advanced distribution management system. The deterministic framework aims to determine the dispatch of DERs at the day-ahead stage to minimize the operational cost, including power purchasing and operational and maintenance costs of DERs. The IGDT-based scheduling scheme aims to maximize the robustness function. This proposed framework is modeled as a MISOCP, which provides the global optimum solution. The uncertainty is addressed using the IGDT framework. In which uncertainty parameters are modeled using the envelop bound model. The DERs considered in this network are PVs, BESSs, and CBs. Since there are two uncertainty parameters, such as PV generation and load demand, present in the system, the proposed problem becomes multi-objective. This multi-objective problem is solved by generating a Pareto-optimal front and selecting the best solution with fuzzy satisfying method..

II. Proposed Day-Ahead Scheduling Scheme

The schematic diagram of the proposed scheduling scheme is shown in Fig. 1. This scheme is used to make the day-ahead dispatch decisions of DERs present in ADN against multiple uncertainties. The operator receives network topology data, forecasts, and grid prices through communication for the proposed scheduling. The proposed IGDT-based scheduling scheme involves three stages. Stage 1 involves determining the base case solution, i.e., the optimum operational cost. Stage 2 involves generating the Pareto optimal front for the robustness functions against multiple uncertainties (PV generation and load demand in this work) by running IGDT-based day-ahead scheduling (DAS) several times. Using the fuzzy satisfying method, the best solution out of the Pareto optimal front will be selected in Stage 3. The optimal decisions will be shared with BESS and CB, and the power purchase schedule will be communicated to the operator. These stages are further discussed in subsequent sections.

A. Deterministic Day-Ahead Scheduling

This section presents the mathematical formulations for the deterministic day-ahead scheduling (DDAS) [8]. In the DDAS framework, all forecasts are assumed to be accurate.

1) Objective Function:

$$\left.\begin{aligned}\min \mathcal{F} = &\sum_{x\in\Omega^{\mathrm{MG}}}\sum_{t\in T}\left[\mathcal{C}_t^{\mathrm{MG}}\,\Delta t\left(\,P_{x,t}^{\mathrm{MG}} + k_q^{\mathrm{MG}} Q_{x,t}^{\mathrm{MG}}\right)\right] + \\ &\sum_{x\in\Omega^{\mathrm{B}}}\sum_{t\in T}\left[\Delta t\,\mathcal{C}^{\mathrm{B}}\left(P_{x,t}^{\mathrm{dis}} + P_{x,t}^{\mathrm{ch}}\right)\right] + \\ &\sum_{x\in\Omega^{\mathrm{CB}}}\sum_{t\in T}\left[\mathcal{C}^{\mathrm{CB}}\left(\mu_{x,t}^{\mathrm{CB,UP}} + \mu_{x,t}^{\mathrm{CB,DN}}\right)\right]\end{aligned}\right\} \tag{1}$$

The objective of DDAS, denoted as $\mathcal{F}$, is to reduce the day-ahead operational expenses of the ADN. Within this function,

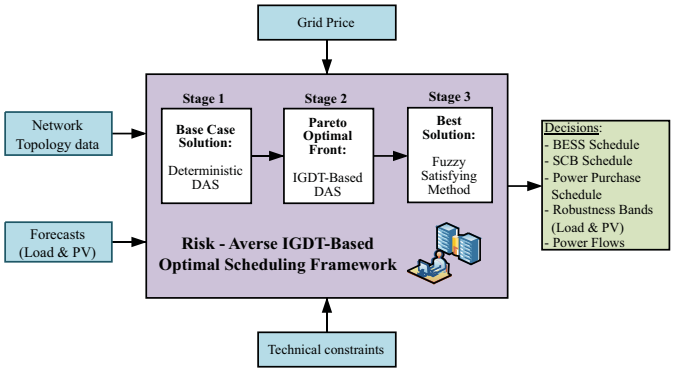

Fig. 1. The IGDT-based optimal scheduling schematic diagram.

the initial component of $\mathcal{F}$ quantifies the expenditure linked to procuring energy from the main grid through the sub-station. Concurrently, the operational and maintenance costs related to the BESS and CB are encompassed by the second and third components of $\mathcal{F}$

2) Constraints:

$$\mu_{x,t}^{\mathrm{ch}} + \mu_{x,t}^{\mathrm{dis}} \le 1,\ \forall t, \forall x \in \Omega^{\mathrm{B}} \tag{2}$$

$$\left.\begin{aligned} 0 \le P_{x,t}^{\mathrm{ch}} \le \mu_{x,t}^{\mathrm{ch}} \overline{S_x^{\mathrm{B}}} \\ 0 \le P_{x,t}^{\mathrm{dis}} \le \mu_{x,t}^{\mathrm{dis}} \overline{S_x^{\mathrm{B}}} \end{aligned}\right\} \forall t, \forall x \in \Omega^{\mathrm{B}} \tag{3}$$

$$\left.\begin{aligned} (P_{x,t}^{\mathrm{ch}})^2 + (Q_{x,t}^{\mathrm{B}})^2 \le (\overline{S_x^{\mathrm{B}}})^2 \\ (P_{x,t}^{\mathrm{dis}})^2 + (Q_{x,t}^{\mathrm{B}})^2 \le (\overline{S_x^{\mathrm{B}}})^2 \end{aligned}\right\} \forall t, \forall x \in \Omega^{\mathrm{B}} \tag{4}$$

$$\left.\begin{aligned} \mathcal{E}_{x,t+1}^{\mathrm{B}} = \mathcal{E}_{x,t}^{\mathrm{B}} + \Delta t\, \lambda_x^{\mathrm{ch}} P_{x,t}^{\mathrm{ch}} - \Delta t\, \lambda_x^{\mathrm{dis}} P_{x,t}^{\mathrm{dis}} \\ \underline{\mathcal{E}_x^{\mathrm{B}}} \le \mathcal{E}_{x,t}^{\mathrm{B}} \le \overline{\mathcal{E}_x^{\mathrm{B}}} \end{aligned}\right\} \forall t, \forall x \in \Omega^{\mathrm{B}} \tag{5}$$

$$\mu_{x,t}^{\mathrm{CB,UP}} + \mu_{x,t}^{\mathrm{CB,DN}} \le 1,\ \forall t, \forall x \in \Omega^{\mathrm{CB}} \tag{6}$$

$$\sum_{t \in T} \left(\mu_{x,t}^{\mathrm{CB,UP}} + \mu_{x,t}^{\mathrm{CB,DN}}\right) \le \overline{N_x^{\mathrm{CB}}},\ \forall x \in \Omega^{\mathrm{CB}} \tag{7}$$

$$\left.\begin{aligned} \tau_{x,t}^{\mathrm{CB}} - \tau_{x,t-1}^{\mathrm{CB}} \le \mu_{x,t}^{\mathrm{CB,UP}} \overline{Y_x^{\mathrm{CB}}} - \mu_{x,t}^{\mathrm{CB,DN}} \\ \tau_{x,t}^{\mathrm{CB}} - \tau_{x,t-1}^{\mathrm{CB}} \ge \mu_{x,t}^{\mathrm{CB,UP}} - \mu_{x,t}^{\mathrm{CB,DN}} \overline{Y_x^{\mathrm{CB}}} \end{aligned}\right\} \forall t, \forall x \in \Omega^{\mathrm{CB}} \tag{8}$$

$$Q_{x,t}^{\mathrm{CB}} = \tau_{x,t}^{\mathrm{CB}} \cdot Q_{x,step}^{\mathrm{CB}},\ \forall t,\ \forall x \in \Omega^{\mathrm{CB}} \tag{9}$$

$$U_{x,t} = V_{x,t}^2/\sqrt{2}, \forall t, \forall x \in \Omega \tag{10}$$

$$\begin{aligned} W_{xy,t}^{\mathrm{R}} &= V_{x,t} V_{y,t} \cos(\theta_{x,t} - \theta_{y,t}) \\ W_{xy,t}^{\mathrm{I}} &= V_{x,t} V_{y,t} \sin(\theta_{x,t} - \theta_{y,t}), \forall t, \forall xy \end{aligned} \tag{11}$$

$$2U_{x,t}U_{y,t} \ge (W_{xy,t}^{\mathrm{R}})^2 + (W_{xy,t}^{\mathrm{I}})^2,\ \forall t, \forall xy \tag{12}$$

$$\left.\begin{aligned} P_{xy,t} = \sqrt{2} G_{xy} U_{x,t} - G_{xy} W_{xy,t}^{\mathrm{R}} - B_{xy} W_{xy,t}^{\mathrm{I}} \\ Q_{xy,t} = -\sqrt{2} B_{xy} U_{x,t} + B_{xy} W_{xy,t}^{\mathrm{R}} - G_{xy} W_{xy,t}^{\mathrm{I}} \end{aligned}\right\} \forall t, \forall xy \tag{13}$$

$$\begin{aligned} &U_{x,t} = 1/\sqrt{2},\ \forall t, \forall x \in \Omega^{\mathrm{MG}} \\ &\underline{V_x}^2/\sqrt{2} \le U_{x,t} \le \overline{V_x}^2/\sqrt{2},\ \forall t, \forall x \in \Omega^{\mathrm{LD}} \end{aligned} \tag{14}$$

$$\left.\begin{aligned} -\overline{V_x V_y} \le W_{xy,t}^{\mathrm{I}} \le \overline{V_x V_y} \\ 0 \le W_{xy,t}^{\mathrm{R}} \le \overline{V_x V_y} \end{aligned}\right\} \forall t, \forall xy \tag{15}$$

$$\left.\begin{aligned} -\overline{P_{xy}} \le P_{xy,t} \le \overline{P_{xy}} \\ -\overline{Q_{xy}} \le Q_{xy,t} \le \overline{Q_{xy}} \end{aligned}\right\} \forall t, \forall xy \tag{16}$$

$$\left.\begin{aligned} P_{x,t}^{\mathrm{MG}} + \left(P_{x,t}^{\mathrm{dis}} - P_{x,t}^{\mathrm{ch}}\right) + \overline{P_{x,t}^{\mathrm{PV}}} - \overline{P_{x,t}^{\mathrm{LD}}} = \sum_{y \in \Omega(x)} P_{xy,t} \\ Q_{x,t}^{\mathrm{MG}} + Q_{x,t}^{\mathrm{B}} + Q_{x,t}^{\mathrm{CB}} - \overline{Q_{x,t}^{\mathrm{LD}}} = \sum_{y \in \Omega(x)} Q_{xy,t} \end{aligned}\right\} \forall t, \forall x \tag{17}$$

$$\begin{aligned} I_{xy,t}^2 &= \sqrt{2}(G_{xy}^2 + B_{xy}^2)(U_{x,t} + U_{y,t} - 2W_{xy,t}^{\mathrm{R}}) \\ &\le \overline{I_{xy}}^2,\ \forall t, \forall xy \end{aligned} \tag{18}$$

Equation (2) governs the charging or discharging of the BESSs within the time interval t. The constraints on the active power of BESSs are outlined in equation (3). Equation (4) illustrates the convex quadratic constraints pertaining to active and reactive power injections from BESSs. At each time interval t, equation (5) defines the energy state of BESSs, encompassing their energy constraints. Equation (6) governs the control of CBs to adjust reactive power compensation during the same time interval t. To ensure that the cumulative switching actions of CBs in a day remain within acceptable limits, equation (7) is enforced, while equation (8) restricts the regulation span of CBs after considering switching variables and the total number of banks. The variables and expressions relevant to the second-order cone programming (SOCP) based power flow model are introduced in equations (10) and (11), with expression (12) embodying the conic constraint. The linear representations of active and reactive power flows for line xy at time interval t are expressed in (13). Equations (14) to (16) define the boundaries for power flow variables. Equation (17) denotes the nodal power balance within the distribution network, and the square of the line current limit ($I_{xy,t}$) can be expressed linearly as shown in equation (18). Collectively, equations (1) through (9) and (12) through (18) constitute the comprehensive formulation of the MISOCP-based DDAS scheme.

B. IGDT-Based Day-Ahead Scheduling

The IGDT is a framework for making decisions in situations where there is uncertainty about the parameters and outcomes of a decision problem [12]. It centers around "info-gaps," representing the level of uncertainty about specific parameters. Rather than estimating outcome probabilities precisely, IGDT aims to identify decision options that perform well across diverse scenarios. Robustness and opportunistic functions are mathematical tools used to evaluate different strategies under uncertainty. Robustness assesses a decision's reliability across various scenarios, while opportunistic functions gauge the potential for exceptional outcomes. These functions help decision-makers align their choices with their objectives and risk tolerance.

In this work, we focus on the IGDT framework to maximize its robustness. It is also known as a risk-averse decision-making scheme. Several methods can model the uncertainty variable in the IGDT framework, but the envelope-bound

model is used in this work due to its simplicity and popularity [11]. The uncertainty parameter $\gamma_{k,t}$, can be formulated as in Eqs. (19) and (20). The expression (20) is nonlinear due to absolute function, which makes the optimization problem non-convex. So, reformulated linearized expressions are given in (21) and (22) [17]. The degree of robustness for the decision vector χ is determined by identifying the maximum range of the uncertainty horizon where all critical system requirements continue to be fulfilled. This can be formulated as in Eqs. (23) and (24). Where $\tilde{R}_z$ is the k^{th} uncertainty parameter's robustness band. $\Psi_{\min}$ is the minimum system requirement.

$$\gamma_{k,t} \in \Gamma_{k,t}(\delta_k, \overline{\gamma_{k,t}}), \quad \forall t, \forall k \in \Upsilon \tag{19}$$

$$\Gamma_{k,t}(\delta_k, \overline{\gamma_{k,t}}) = \left| \frac{\gamma_{k,t} - \overline{\gamma_{k,t}}}{\overline{\gamma_{k,t}}} \right| \leq \delta_k \tag{20}$$

$$\left(\frac{\gamma_{k,t} - \overline{\gamma_{k,t}}}{\overline{\gamma_{k,t}}} \right) \leq \delta_k \tag{21}$$

$$-\left(\frac{\gamma_{k,t} - \overline{\gamma_{k,t}}}{\overline{\gamma_{k,t}}} \right) \leq \delta_k \tag{22}$$

$$\tilde{R}_z = \max_{\delta_k} \{\delta_k\}, \quad \forall k \in \Upsilon \tag{23}$$

$$\min\{\Psi(\chi, \gamma_1, \gamma_2, ..., \gamma_n)\} \geq \Psi_{\min} \tag{24}$$

$\tilde{\mathcal{F}}$ in the below expression shows the forecasted cost obtained from the DDAS scheme by assuming load demand and PV generation forecasts are accurate.

$$\tilde{\mathcal{F}} = \min_{\tilde{\chi}} \mathcal{F}(\overline{P^{\mathrm{PV}}}, \overline{S^{\mathrm{LD}}}) \tag{25}$$

St: (2)-(9), (12)-(18)

The expression in (26) shows the minimum system requirement, $\mathcal{F}_{\mathrm{MC}}$. In which ξ is the permissible increase in the operational cost. The ξ can be selected based on the requirement and experience of the operator.

$$\mathcal{F}(P^{\mathrm{PV}}, S^{\mathrm{LD}}) \leq \mathcal{F}_{\mathrm{MC}} \tag{26}$$

$$\mathcal{F}_{\mathrm{MC}} = (1 + \xi)\tilde{\mathcal{F}} \tag{27}$$

In this work, we considered two uncertainty parameters, i.e., PV generation and load demand. The objective function, OF, is to maximize the robustness against all two uncertain variables. The maximum risk (increase in operational cost) occurs when PV generation reduces (30) and load demand increases (31). Here, it is trying to set the decision variable χ to prepare for the worst condition, which may cause more risk, and make sure that the minimum requirement (26) is always met. Eq. (32) represents the power balance at every node with actual values ($P^{\mathrm{PV}}_{x,t}, P^{\mathrm{LD}}_{x,t}, Q^{\mathrm{LD}}_{x,t}$).

$$\max_{\tilde{\chi}} OF \tag{28}$$

$$OF = \min(\delta_{\mathrm{PV}} \text{ or } \delta_{\mathrm{LD}}) \tag{29}$$

$$P^{\mathrm{PV}}_{x,t} = \overline{P^{\mathrm{PV}}_{x,t}}(1 - \delta_{\mathrm{PV}}), \forall x \in \Omega^{\mathrm{PV}}, \forall t \in T \tag{30}$$

$$S^{\mathrm{LD}}_{x,t} = \overline{S^{\mathrm{LD}}_{x,t}}(1 + \delta_{\mathrm{LD}}), \forall x \in \Omega^{\mathrm{LD}}, \forall t \in T \tag{31}$$

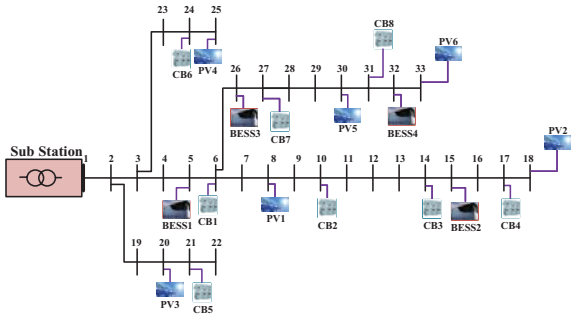

Fig. 2. Standard IEEE 33-bus distribution network integrated with DERs.

$$\left.\begin{aligned} P^{\mathrm{MG}}_{x,t} + \left(P^{\mathrm{dis}}_{x,t} - P^{\mathrm{ch}}_{x,t}\right) + P^{\mathrm{PV}}_{x,t} - P^{\mathrm{LD}}_{x,t} &= \sum_{y \in \Omega(x)} P_{xy,t} \\ Q^{\mathrm{MG}}_{x,t} + Q^{\mathrm{B}}_{x,t} + Q^{\mathrm{CB}}_{x,t} - Q^{\mathrm{LD}}_{x,t} &= \sum_{y \in \Omega(x)} Q_{xy,t} \end{aligned}\right\} \forall t, \forall x \tag{32}$$

The proposed formulation becomes multi-objective optimization since the OF has two objectives. To find the best solution, form a Pareto optimal front [18], and a fuzzy satisfying method is used to find the best solution from the Pareto optimal front [18]. The procedure to solve multi-objective optimization for this problem (two objectives) is explained in Algorithm 1. It is to be noted that this technique can be applied to solving multi-objective functions having more than two objectives.

Algorithm 1: : Procedure to Solve Multi-Objective Optimization Problem

1. Initially, solve the DDAS scheme (25) and find out the base case solution $\tilde{\mathcal{F}}$.
2. For a value of ξ, take one objective among δ_{PV} and δ_{LD} and solve the IGDT-base DAS to determine their maximum value.
3. Add one of the objective functions as a constraint in the optimization problem. In this work, $\delta_{\mathrm{LD}} \leq \epsilon$.
4. By varying ϵ, from $\delta^{\max}_{\mathrm{LD}}$ to $\delta^{\min}_{\mathrm{LD}}$, run proposed framework for maximizing δ_{PV}.
5. δ_{PV} vs δ_{LD} gives the Pareto optimal front.
6. Determine the linear membership function value, $\phi_{g_j}(Z_i)$, from the multiple solutions of the Pareto optimal front.
7. Find the best solution by calculating the solution with minimum dissatisfaction of all objective functions from (34).

$$\phi_{g_j}(Z_i) = \begin{cases} 1, & g_j(Z_i) > g^{\max}_j \\ \frac{g^{\min}_j - g_j(Z_i)}{g^{\min}_j - g^{\max}_j}, & g^{\min}_j \leq g_j(Z_i) \leq g^{\max}_j \\ 0, & g_j(Z_i) < g^{\min}_j \end{cases} \tag{33}$$

$$\max_{i=1:\Lambda_p} \min_{j=1:\Lambda_o} (\phi_{g_j}(Z_i)) \tag{34}$$

III. CASE STUDY

A. Specifications of Test System

The proposed scheduling scheme is programmed in GAMS software on a personal computer with an i7, 3.2 GHz, and 16

TABLE I
DETAILS OF DIFFERENT ELEMENTS IN 33-BUS SYSTEM

Type	Location	Details of each element
PV	8, 18, 20, 25, 30, 33.	Rating = 0.6 MW.
CB	6, 10, 14, 17, 21, 24, 27, 31.	$Q^{\mathrm{CB}}_{x,step} = 0.05$ MVAr, $\overline{\Psi^{\mathrm{CB}}_x} = 5$, $\overline{N^{\mathrm{CB}}_x} = 5, \mathcal{C}^{\mathrm{CB}}_x = 0.5\$$.
BESS	5, 15, 26, 32.	$\overline{S^{\mathrm{B}}_x} = 0.2$ MVA, $\overline{\mathcal{E}^{\mathrm{B}}_x} = 0.45$ MWh, $\underline{\mathcal{E}^{\mathrm{B}}_x} = 0.05$ MWh, $\lambda^{\mathrm{ch}}_x = (1/\lambda^{\mathrm{dis}}_x) = 0.9, \mathcal{C}^{\mathrm{B}}_x = 5\$$/MW.
Other	-	$k^{MG}_q = 0.05$, $\overline{P_{xy}}$ =5 pu, $\overline{I_{xy}} = 5$ pu, $\underline{V_x} = 0.9$ pu, $\overline{V_x} = 1.1$pu.

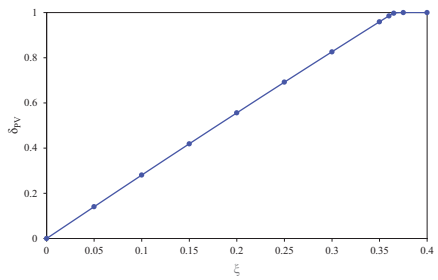

Fig. 3. Variation of robustness versus the variation of ξ against PV generation uncertainty.

GB of RAM and solved with a GUROBI solver. A modified IEEE 33-bus system used to validate proposed scheduling is shown in Fig. 2. The necessary data is obtained from [8]. The details of different elements connected to IEEE 33-bus are presented in Table I. The minimum and maximum limits of upper grid active/reactive power are 0 and 6 pu, respectively. The normalized forecast data corresponding to PV generation, load demand, and main grid price is obtained from [8]. In this work, the price received from the grid is assumed to be accurate.

B. Results and Discussion

In this work, four different strategies are discussed to validate the proposed framework. The details regarding these four strategies are given below:
Strategy 1: In this strategy, forecasts of PV generation and load demand are assumed to be accurate.
Strategy 2: Only PV generation forecast uncertainty is considered, and the load demand forecast is assumed to be accurate.
Strategy 3: Only load demand forecast uncertainty is considered, and the PV generation forecast is assumed to be accurate.
Strategy 4: PV generation and load demand forecast uncertainty are considered in this strategy.

The optimal objective function of Strategy 1, which is the base case value, is obtained as \$5951.32 by running the DDAS framework. This base case value in stage 1 is supplied to stage 2.

Strategy 2 optimizes the robustness function against PV generation forecasting uncertainty. The optimal robustness value δ_{PV} versus varying ξ value is plotted in Fig. 3. We can observe the linear relationship between δ_{PV} and ξ from ξ 0 to 0.365. After ξ is above 0.365, the robustness is always unity. These results show that if the operator chooses to increase

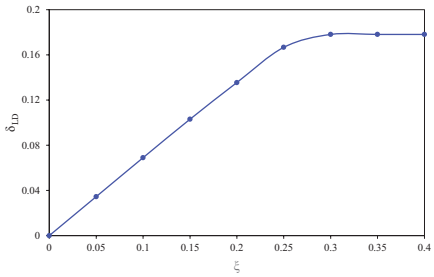

Fig. 4. Variation of robustness versus the variation of ξ against load demand uncertainty.

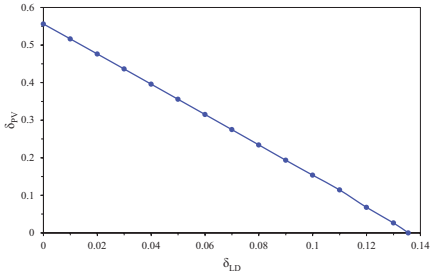

Fig. 5. Pareto optimal front of robustness against PV generation and load demand uncertainty.

ADN's operational costs by 36.5%, the distribution network is robust against PV generation uncertainty.

Strategy 3 optimizes the robustness function against load demand forecasting uncertainty. The optimal robustness value δ_{LD} versus varying ξ value is plotted in Fig. 4. Like Strategy 2, δ_{LD} is linearly varying with ξ until its value is 0.25. After ξ is above 0.3, the robustness always equals 0.1781. These results show that, even if the operator is ready to increase ADN's operational cost, the robustness against load demand is not increasing. This is due to security limits such as voltage and line current carrying.

Strategy 4 is a multi-objective optimization problem since the objective is to optimize the robustness functions of PV generation and load demand simultaneously. First, we generated the Pareto optimal front and selected the best solution using the fuzzy satisfying method according to Algorithm 1. For ξ is equal to 0.2, the optimum values of δ_{LD} and δ_{LD} are 0.2748 and 0.07 respectively. The total computational time required to generate the optimal front is 623.52 sec. So, it is feasible for the operator to run the proposed multi-objective IGDT-based optimal scheduling framework for any value of ξ since the decisions are taken at the day-ahead stage. The operational cost will increase if the operator wants higher robustness against uncertainty.

The minimum voltage in the modified IEEE 33-bus ADN at every time interval for all four strategies is plotted in Fig. 6. The voltage profile is best in Strategy 1, but it is not advisable to implement it in practical scenarios since uncertainty is not addressed in this strategy. The total active power injection from all four BESSs into ADN at every time interval is plotted in Fig. 7. Similarly, the sum of reactive power from all eight CBs and four BESSs are plotted in Fig. 8 (a) and 8 (b), respectively.

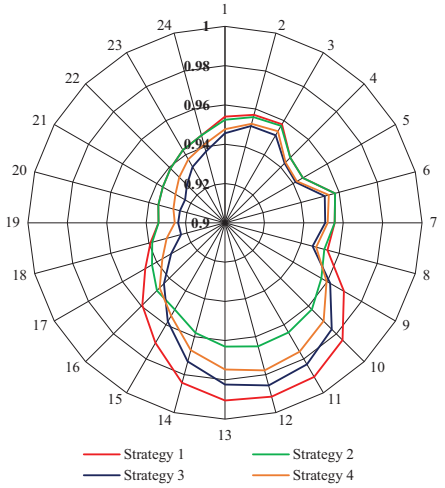

Fig. 6. The hourly minimum voltage of four different strategies in the system.

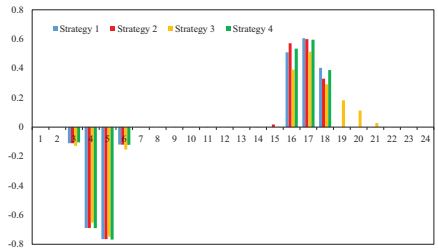

Fig. 7. The total active power injection from all four BESSs in the four different strategies.

IV. Conclusion

An optimal day-ahead scheduling for ADN to maximize the robustness against uncertainty is proposed in this paper. The multiple uncertainties (PV generation and load demand) present in ADN are addressed through the IGDT framework. The overall scheme is formulated as a multi-objective MISOCP problem. The multi-objective problem is solved by forming the Pareto optimal front and selecting the best solution through the fuzzy satisfaction method. The proposed framework results on the modified IEEE 33-bus DN for four strategies are discussed. The voltage profile is best in Strategy 1, but it is not advisable to implement it in practical scenarios since uncertainty is not addressed in this strategy. The results show that the robustness value increases with an increase in the minimum requirement function value. In this work, the computational time required to form a Pareto optimal front is 623.52 sec. Therefore, the operator can run the problem several times by varying the permissible increase in the operational cost and make decisions from these optimal robustness values of PV generation and load demand. Therefore, the proposed framework is robust against uncertainty, easy to implement, and requires less computational time.

Fig. 8. Total reactive power injection from (a) BESSs (b)CBs.

References

[1] K. Mongird, V. V. Viswanathan, P. J. Balducci, M. J. E. Alam, V. Fotedar, V. S. Koritarov, and B. Hadjerioua, "Energy storage technology and cost characterization report," tech. rep., Pacific Northwest National Lab.(PNNL), Richland, WA (United States), 2019.

[2] S. Golshannavaz, S. Afsharnia, and F. Aminifar, "Smart distribution grid: Optimal day-ahead scheduling with reconfigurable topology," *IEEE Transactions on Smart Grid*, vol. 5, no. 5, pp. 2402–2411, 2014.

[3] Y.-R. Lee, H.-J. Kang, and M.-K. Kim, "Optimal operation approach with combined bess sizing and pv generation in microgrid," *IEEE Access*, vol. 10, pp. 27453–27466, 2022.

[4] S. Krishna, D. M, and S. R, "Optimal scheduling of distribution system with pv and battery energy storage system," in *2022 IEEE Kansas Power and Energy Conference (KPEC)*, pp. 1–6, 2022.

[5] R. Zafar, J. Ravishankar, J. E. Fletcher, and H. R. Pota, "Optimal dispatch of battery energy storage system using convex relaxations in unbalanced distribution grids," *IEEE Transactions on Industrial Informatics*, vol. 16, no. 1, pp. 97–108, 2020.

[6] S.-K. Kim, J.-Y. Kim, K.-H. Cho, and G. Byeon, "Optimal operation control for multiple besss of a large-scale customer under time-based pricing," *IEEE Transactions on Power Systems*, vol. 33, no. 1, pp. 803–816, 2018.

[7] Y. Zheng, J. Zhao, Y. Song, F. Luo, K. Meng, J. Qiu, and D. J. Hill, "Optimal operation of battery energy storage system considering distribution system uncertainty," *IEEE Transactions on Sustainable Energy*, vol. 9, no. 3, pp. 1051–1060, 2018.

[8] K. Vemalaiah, D. K. Khatod, and N. P. Padhy, "Optimal day-ahead scheduling for active distribution network considering uncertainty," in *2022 IEEE International Conference on Power Electronics, Drives and Energy Systems (PEDES)*, pp. 1–6, IEEE, 2022.

[9] K. Wang, C. Wang, Z. Zhang, and X. Wang, "Multi-timescale active distribution network optimal dispatching based on smpc," *IEEE Transactions on Industry Applications*, vol. 58, no. 2, pp. 1644–1653, 2022.

[10] W. Kong, Z. Y. Dong, D. J. Hill, F. Luo, and Y. Xu, "Short-term residential load forecasting based on resident behaviour learning," *IEEE Transactions on Power Systems*, vol. 33, no. 1, pp. 1087–1088, 2018.

[11] M. Majidi, B. Mohammadi-Ivatloo, and A. Soroudi, "Application of information gap decision theory in practical energy problems: A comprehensive review," *Applied Energy*, vol. 249, pp. 157–165, 2019.

[12] Y. Ben-Haim, *Info-gap decision theory: decisions under severe uncertainty*. Elsevier, 2006.

[13] M. Salimi, M.-A. Nasr, S. H. Hosseinian, G. B. Gharehpetian, and M. Shahidehpour, "Information gap decision theory-based active distribution system planning for resilience enhancement," *IEEE Transactions on Smart Grid*, vol. 11, no. 5, pp. 4390–4402, 2020.

[14] M. Izadi, S. H. Hosseinian, S. Dehghan, A. Fakharian, and N. Amjady, "Resiliency-oriented operation of distribution networks under unexpected wildfires using multi-horizon information-gap decision theory," *Applied Energy*, vol. 334, p. 120536, 2023.

[15] A. Ahmadi, A. Esmaeel Nezhad, P. Siano, B. Hredzak, and S. Saha, "Information-gap decision theory for robust security-constrained unit commitment of joint renewable energy and gridable vehicles," *IEEE Transactions on Industrial Informatics*, vol. 16, no. 5, pp. 3064–3075, 2020.

[16] A. O'Connell, A. Soroudi, and A. Keane, "Distribution network operation under uncertainty using information gap decision theory," *IEEE Transactions on Smart Grid*, vol. 9, no. 3, pp. 1848–1858, 2018.

[17] M. Asghari, A. M. Fathollahi-Fard, S. Mirzapour Al-E-Hashem, and M. A. Dulebenets, "Transformation and linearization techniques in optimization: A state-of-the-art survey," *Mathematics*, vol. 10, no. 2, p. 283, 2022.

[18] A. Soroudi, *Power system optimization modeling in GAMS*, vol. 78. Springer, 2017.